

Article

Chloranilato-Based Layered Ferrimagnets with Solvent-Dependent Ordering Temperatures

Cristian Martínez-Hernández, Samia Benmansour *  and Carlos J. Gómez-García * 

Instituto de Ciencia Molecular (ICMol), Departamento de Química Inorgánica, Universidad de Valencia, C/Catedrático José Beltrán 2, 46980 Paterna, Spain; christian.martinez@uv.es

* Correspondence: sam.ben@uv.es (S.B.); carlos.gomez@uv.es (C.J.G.-G.);

Tel.: +34-963-544-423 (S.B. & C.J.G.-G.); Fax: +34-963-543-273 (S.B. & C.J.G.-G.)

Received: 2 May 2019; Accepted: 28 May 2019; Published: 4 June 2019



Abstract: We report the synthesis and the characterization of six new heterometallic chloranilato-based ferrimagnets formulated as $(\text{NBu}_4)[\text{MnCr}(\text{C}_6\text{O}_4\text{Cl}_2)_3] \cdot n\text{G}$ with $n = 1$ for $\text{G} = \text{C}_6\text{H}_5\text{Cl}$ (**1**), $\text{C}_6\text{H}_5\text{I}$ (**3**), and $\text{C}_6\text{H}_5\text{CH}_3$ (**4**); $n = 1.5$ for $\text{G} = \text{C}_6\text{H}_5\text{Br}$ (**2**) and $n = 2$ for $\text{G} = \text{C}_6\text{H}_5\text{CN}$ (**5**) and $\text{C}_6\text{H}_5\text{NO}_2$ (**6**); $(\text{C}_6\text{O}_4\text{Cl}_2)^{2-} = 1,3\text{-dichloro},2,5\text{-dihydroxy}-1,4\text{-benzoquinone}$ dianion. The six compounds are isostructural and show hexagonal honeycomb layers of the type $[\text{MnCr}(\text{C}_6\text{O}_4\text{Cl}_2)_3]^-$ alternating with layers containing the NBu_4^+ cations. The hexagons are formed by alternating Mn(II) and Cr(III) connected by bridging bis-bidentate chloranilato ligands. The benzene derivative solvent molecules are located in the hexagonal channels (formed by the eclipsed packing of the honeycomb layers) showing $\pi\text{-}\pi$ interactions with the anilato rings. The six compounds behave as ferrimagnets with ordering temperatures in the range 9.8–11.2 K that can be finely tuned by the donor character of the benzene ring and by the number of solvent molecules inserted in the hexagonal channels. The larger the electron density on the aromatic ring and the larger the number of solvent molecules are, the higher T_c is. The only exception is provided by toluene, where the formation of H-bonds might be at the origin of weaker $\pi\text{-}\pi$ interactions observed in this compound.

Keywords: two-dimensional (2D) ferrimagnets; chloranilato; heterometallic layers; honeycomb layers; molecule-based magnets

1. Introduction

One of the main advantages of molecule-based magnets is the possibility to modulate or tune the properties of the magnets by simply changing or modifying the building blocks used to prepare them [1]. This strategy led, at the end of last century, to the synthesis of different series of molecule-based magnets whose ordering temperatures and coercive fields could be modified with ease. A typical example is provided by the series of cyano-bridged heterometallic compounds formulated as $\text{A}_x\text{M}_y[\text{M}'(\text{CN})_6]_z \cdot n\text{H}_2\text{O}$, where A is a monovalent cation, and M and M' are trivalent or divalent transition metal ions [2–4]. In this series, the magnetic exchange through the CN bridge can be modulated [5,6] by changing A, M, and M' to obtain materials with interesting magnetic properties as photomagnetism [7–9], single molecule magnets [10,11], and even magnetic order above room temperature [12]. Another family of molecule-based magnets whose properties can be easily modified by changing the constituent metallic atoms is the series of oxalato-based two-dimensional (2D) magnets formulated as $(\text{A})[\text{M}^{\text{II}}\text{M}^{\text{III}}(\text{C}_2\text{O}_4)_3]$ ($\text{A}^+ = \text{monocation}$; $\text{M}^{\text{II}} = \text{Mn, Fe, Co, Ni, Cu, } \dots$; $\text{M}^{\text{III}} = \text{Fe, Cr, } \dots$; $\text{C}_2\text{O}_4^{2-} = \text{oxalate dianion}$, Figure 1b) that show ferro-, ferri-, or canted antiferromagnetic ordering with T_c ranging from 6 K to 48 K depending on M(II) and M(III) [13–22].

A third and recent example is the series of anilato-based heterometallic 2D honeycomb magnets formulated as $(\text{A})[\text{M}^{\text{II}}\text{M}^{\text{III}}(\text{C}_6\text{O}_4\text{X}_2)_3] \cdot \text{G}$, where A^+ is a monocation (see Table 1); M(II) and M(III) are transition metal ions as Mn(II), Fe(II), Cr(III), and Fe(III), G may be many different solvent

molecules (see Table 1), and $C_6O_4X_2^{2-}$ is the 1,3-disubstituted-2,5-dihydroxy- 1,4-benzoquinone dianion (with $X = H, Cl, Br, NO_2, \dots$ Figure 1a), known as anilato-type ligands [23]. This family of magnets shows a honeycomb (6,3)-2D structure with the same topology as the oxalato ones and, as in the oxalato family, it is also possible to change the magnetic properties by simply changing the building blocks [23,24]. Albeit, there are three important differences between these two series; the first difference is observed in the sign of the magnetic coupling—it is always antiferromagnetic in the anilato-based compounds, whereas it may be ferro- or antiferromagnetic depending on the metal ions, for the oxalato series. This fact precludes the presence of magnetic ordering in the homo-metallic anilato-based lattices but not in the hetero-metallic ones, where long range ferrimagnetic is observed when the spin states of the metal ions are different [Mn(II)Cr(III) and Fe(II)Fe(III), see Table 1]. The second difference is the rigidity of the oxalato ligand (Figure 1b) in contrast to the anilato ligand that can be easily modified by changing the X group ($X = H, F, Cl, Br, I, CH_3, Cl/CN, NO_2, \dots$) [25]. This change has already allowed a tuning of the ordering temperatures in the series of compounds $(NBu_4)[MnCr(C_6O_4X_2)_3]$ ($X = H, Cl, Br,$ and I) [23]. The third important difference is the size; the hexagonal cavities of the honeycomb structure are twice as large in the anilato-based compounds and, when packed in an eclipsed way, originate hexagonal channels with BET areas of up to $1440 \text{ m}^2/\text{g}$ [26]. These hexagonal channels may be filled with solvent molecules (in contrast to the oxalato-based compounds) that can be easily removed, giving rise, in some cases, to important changes in the magnetic properties. Thus, in compound $(NMe_2H_2)_2[Fe_2(C_6O_4Cl_2)_3] \cdot 2H_2O \cdot 6DMF$, the removal of the solvent molecules results in a decrease of the ordering temperature from 80 to 26 K [27]. In compound $(Et(i-Pr)_2NH)[MnCr(C_6O_4Br_2)_3] \cdot H_2O \cdot 0.5CHCl_3$, the removal of the solvent molecules changes the magnetic behavior (the solvated compound is a metamagnet with a critical field of 490 mT at 2 K, whereas the de-solvated phase is a ferrimagnet with $T_c = 9 \text{ K}$) [28].

The possibility to change the magnetic properties (ordering temperatures, magnetic behavior, or critical and coercive fields) by simply changing the solvent molecules is, therefore, a very appealing strategy to modulate T_c in these series of 2D magnets. Furthermore, when using lanthanoids as metal ions, the solvent molecules also play a key structural role in these (6,3)-2D lattices [24,29–38].

In this context, we have recently initiated a detailed study of the role played by the solvent molecules located in the hexagonal channels in the structure and the magnetic properties of these 2D magnets formulated as $(A)[M^{II}M^{III}(C_6O_4X_2)_3] \cdot G$. To perform this study, we have initially selected Mn(II) and Cr(III) as M^{II} and M^{III} , since this couple of metal ions crystallizes more easily (Table 1). We have selected $A = NBu_4^+$ as the cation and chloranilato as the ligand ($X = Cl$), and we have focused on a series of benzene derivative solvent molecules (C_6H_5X with $X = Cl, Br, I, CH_3, CN,$ and NO_2), since they seem to play a template role that facilitates the crystallization of these 2D lattices. With this idea in mind, we have prepared the series of compounds formulated as $(NBu_4)[MnCr(C_6O_4Cl_2)_3] \cdot n C_6H_5X$ with $n/X = 1/Cl$ (1), $1.5/Br$ (2), $1/I$ (3), $1/CH_3$ (4), $2/CN$ (5), and $2/NO_2$ (6). This series of compounds are solvates since they are isostructural and only differ in the solvent molecules. They present the structure of compound $(NBu_4)[MnCr(C_6O_4Br_2)_3] \cdot C_6H_5Br \cdot 0.5H_2O$ (A) [39] and show a fine modulation of the ordering temperatures in the range 9.8–11.2 K depending on the electronic properties of the benzene derivative molecule and on the number of solvent molecules inserted in the channels.

Here, we present the chemical and the magnetic characterization of the six compounds and show that it is possible to fine-tune the ordering temperatures with a simple change of the solvent molecules.

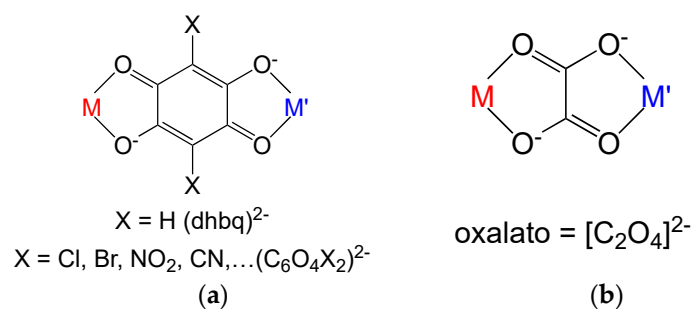


Figure 1. (a) The anilato family of ligands (C₆O₄X₂)²⁻ showing the typical bis-bidentate coordination mode also shown by the oxalato ligand (b).

Table 1. Magnetic properties of all the structurally characterized hetero-metallic layered compounds of the type (A)[M^{II}M^{III}(C₆O₄X₂)₃](solvent).

CCDC	Formula	Packing	Space Group	T _c (K)	H _{coer} (mT) ^a	Ref.
MIRFEA	[(H ₃ O)(phz) ₃][MnCr(C ₆ O ₄ Cl ₂) ₃ (H ₂ O)] ^b	eclipsed	P3	5.5	19.4	[23]
MIRFIE	[(H ₃ O)(phz) ₃][MnCr(C ₆ O ₄ Br ₂) ₃]·2H ₂ O·2CH ₃ COCH ₃	eclipsed	P-31m	6.3	34.0	[23]
MIRFOK	[(H ₃ O)(phz) ₃][MnFe(C ₆ O ₄ Br ₂) ₃]·H ₂ O	eclipsed	P-31m	-	-	[23]
MIRFUQ	(NBu ₄)[MnCr(C ₆ O ₄ Cl ₂) ₃]	alternated	C2/c	5.5	11.8	[23]
HOWHAE	[Fe(sal ₂ -trien)][MnCr(C ₆ O ₄ Cl ₂) ₃]·0.5CH ₂ Cl ₂ ·CH ₃ OH·0.5H ₂ O·5CH ₃ CN	alternated	C222 ₁	10.0	35	[40]
HOWHEI	[Fe(4-OH-sal ₂ -trien)][MnCr(C ₆ O ₄ Cl ₂) ₃]·G	alternated	P6 ₁ 22	10.4	87	[40]
HOWHIM	[Fe(sal ₂ -epe)][MnCr(C ₆ O ₄ Br ₂) ₃]·4CH ₃ CN	alternated	P2 ₁ /c	10.2	10	[40]
HOWHOS	[Fe(5-Cl-sal ₂ -trien)][MnCr(C ₆ O ₄ Br ₂) ₃]·CH ₂ Cl ₂ ·CH ₃ OH·4H ₂ O·1.5CH ₃ CN	alternated	P2 ₁ /c	9.8	66	
MUMKUC	[Fe(acac ₂ -trien)][MnCr(C ₆ O ₄ Cl ₂) ₃]·2CH ₃ CN	alternated	C2/c	10.8	65	[41]
MUMLAJ	[Fe(acac ₂ -trien)][MnCr(C ₆ O ₄ Br ₂) ₃]·2CH ₃ CN	alternated	C2/c	11.1	77	[41]
MUMLEN	[Ga(acac ₂ -trien)][MnCr(C ₆ O ₄ Br ₂) ₃]·2CH ₃ CN	alternated	C2/c	11.6	72	[41]
SEPLAD	(Me ₂ NH ₂)[MnCr(C ₆ O ₄ Br ₂) ₃]·2H ₂ O	alternated	P-31c	7.9	90	[28]
SEPLEH	(Et ₂ NH ₂)[MnCr(C ₆ O ₄ Br ₂) ₃]	alternated	P-31c	8.9	100	[28]
SEQCID	(Et ₃ NH)[MnCr(C ₆ O ₄ Cl ₂) ₃]	alternated	P-31c	8.0	150	[28]
SEPROX	(Et(i-Pr) ₂ NH)[MnCr(C ₆ O ₄ Br ₂) ₃]	alternated	P-31c	9.0	4 ^c	[28]
1910770	(NBu ₄)[MnCr(C ₆ O ₄ Br ₂) ₃]·C ₆ H ₅ Br·0.5H ₂ O	eclipsed	P2 ₁	9.5	33	[39]
QEFPOJ	[(H ₃ O)(phz) ₃][FeFe(C ₆ O ₄ Cl ₂) ₃]·12H ₂ O ^d	eclipsed	P-31m	2.4	1.0	[42]
QEFPID	[(H ₃ O)(phz) ₃][FeFe(C ₆ O ₄ Br ₂) ₃]·12H ₂ O ^d	eclipsed	P-31m	2.1	1.0	[42]
NIHJEW01	[C(N ₂ H ₃) ₃][FeFe(C ₆ O ₄ (CN)Cl) ₃]·29H ₂ O ^d	eclipsed	P3	4.0	6	[43]
1909314	(NBu ₄)[MnCr(C ₆ O ₄ Cl ₂) ₃ (C ₆ H ₅ CHO)]·C ₆ H ₆ ^b	eclipsed	P2 ₁	7.0	7.6	[44]
1909315	(NBu ₄)[MnCr(C ₆ O ₄ Br ₂) ₃ (C ₆ H ₅ CHO)]·C ₆ H ₆ ^b	eclipsed	P2 ₁	6.7	10	[44]
1909316	(NBu ₄)[MnCr(C ₆ O ₄ Cl ₂) ₃ (C ₆ H ₅ CHO)]·C ₆ H ₅ CHO ^b	eclipsed	P2 ₁	6.8	5.0	[44]
1909317	(NBu ₄)[MnCr(C ₆ O ₄ Br ₂) ₃ (C ₆ H ₅ CHO)]·C ₆ H ₅ CHO ^b	eclipsed	P2 ₁	6.7	20	[44]

^a at 2 K; ^b the H₂O or C₆H₅CHO molecule is coordinated to the Mn ion; ^c A solvated phase of this compound is metamagnetic with a critical field at 2 K of 490 mT. ^d These compounds are homo-metallic but show two different oxidation states.

2. Results and Discussion

2.1. Syntheses of the Complexes

The six compounds were synthesized by carefully layering solutions containing the precursor [Cr(C₆O₄Cl₂)₃]³⁻ anion and Mn(II) ions with the corresponding benzene derivative solvents. In all cases, an intermediate layer was needed to slow down the crystallization process and prevent the formation of amorphous or low quality crystalline materials. All the attempts to obtain good quality

single crystals failed, although the X-ray powder diffractograms showed that they are all isostructural to the closely related compound $(\text{NBu}_4)[\text{MnCr}(\text{C}_6\text{O}_4\text{Br}_2)_3]\cdot\text{C}_6\text{H}_5\text{Br}\cdot 0.5\text{H}_2\text{O}$ (A) [39].

2.2. FT-IR Spectra

As expected, the six compounds showed very similar IR spectra (Figure 2). The only differences corresponded to the bands associated with the solvent molecules. Table 2 lists the main bands and their assignments. The FT-IR spectra in all cases confirmed the presence of the corresponding solvent molecules ($\text{C}_6\text{H}_5\text{Cl}$ in 1, $\text{C}_6\text{H}_5\text{Br}$ in 2, $\text{C}_6\text{H}_5\text{I}$ in 3, $\text{C}_6\text{H}_5\text{CH}_3$ in 4, $\text{C}_6\text{H}_5\text{CN}$ in 5, and $\text{C}_6\text{H}_5\text{NO}_2$ in 6), in agreement with the chemical and the thermo-gravimetric analysis.

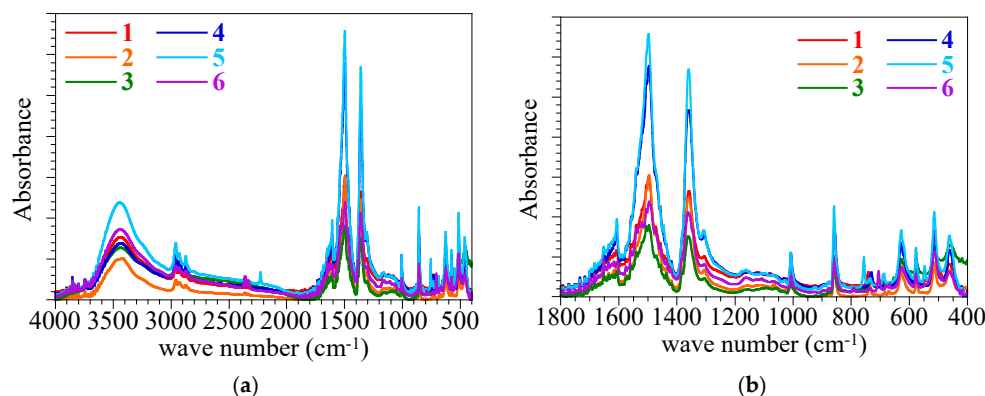


Figure 2. (a) Absorbance FT-IR spectra of compounds 1–6 in the range 4000–400 cm^{-1} (a) and 1800–400 cm^{-1} (b).

Table 2. Main IR bands (cm^{-1}) and their assignments for compounds 1–6.

Band	1 ($\text{C}_6\text{H}_5\text{Cl}$)	2 ($\text{C}_6\text{H}_5\text{Br}$)	3 ($\text{C}_6\text{H}_5\text{I}$)	4 ($\text{C}_6\text{H}_5\text{CN}$)	5 ($\text{C}_6\text{H}_5\text{CH}_3$)	6 ($\text{C}_6\text{H}_5\text{NO}_2$)
$\nu(\text{C-H})$	2959	2959	2960	2962	2960	2963
	2929	2929	2928	2931	2928	2931
	2873	2873	2873	2873	2873	2873
$\nu(\text{C}\equiv\text{N})^1$	-	-	-	2227	-	-
$\nu(\text{C}=\text{O})$	1609	1606	1607	1607	1607	1606
$\nu(\text{N-O})_{\text{as}}^1$	-	-	-	-	-	1520
$\nu(\text{C}=\text{C})^1$	1506	1506 *	1505	1507 *	1505 *	1505
$\nu(\text{C}=\text{C}) + \nu(\text{C-O})$	1495	1496	1496	1497	1496	1495
$\delta(\text{C-H})$	1383	1382	1383	1383 *	1383 *	1383
$\nu(\text{C-C}) + \nu(\text{C-O})$	1360	1362	1361	1360	1359	1361
$\nu(\text{N-O})_{\text{s}}^1$	-	-	-	-	-	1344 *
$\nu(\text{C-N})^1$	-	-	-	-	-	877
$\delta(\text{C-X})$	860	858	858	858	858	857
$\nu(\text{C-Cl})^1$	740	-	-	-	-	-
$\delta(\text{C-H})^1$	700	737	730	734	730	705
	684	682	685	687	693	683
$\rho(\text{C-X})$	577	576	576	577	576	577

* shoulder; ¹ Bands corresponding to the solvent molecules.

2.3. Thermogravimetric Analysis

The thermogravimetric analysis of compounds 1–6 (Figure 3) showed an initial weight loss with a plateau in the range *ca.* 200–290 °C depending on the sample (Table 3). This weight loss corresponded to the release of the benzene derivative solvent molecules. The experimental weight loss (Table 3) indicated that compounds 1, 3, and 4 contained one solvent molecule (C_6H_5Cl in 1, C_6H_5I in 3, and $C_6H_5CH_3$ in 4), whereas compound 2 contained 1.5 C_6H_5Br molecules and compounds 5 and 6 contained two solvent molecules (C_6H_5CN in 5 and $C_6H_5NO_2$ in 6). These values are in agreement with the elemental analysis in all cases (see experimental section). We can, therefore, conclude that the used solvents (C_6H_5Cl , C_6H_5Br , C_6H_5I , $C_6H_5CH_3$, C_6H_5CN , and $C_6H_5NO_2$) entered in the structures of compounds 1–6 (as observed in the IR spectra), and that compounds 1, 3, and 4 contain one solvent molecule, compound 2 contains *ca.* 1.5, and compounds 5 and 6 contain around two solvent molecules per formula. At higher temperatures (around 350 °C), all compounds showed an abrupt weight loss corresponding to the decomposition and the release of the chloranilate ligand. As can be seen in the derivative plot, compound 4 needed a higher temperature (around 300 °C) to release the toluene molecule, suggesting that this molecule has a stronger interaction with the 2D lattice (probably due to the formation of H-bonds, as already observed in other anilato-based lattices) [34].

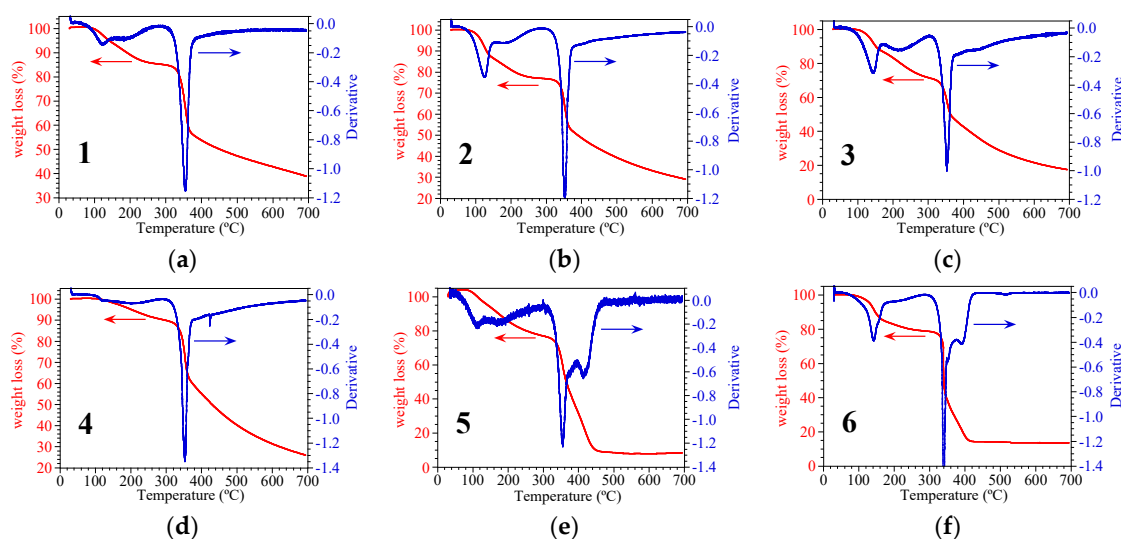


Figure 3. Thermogravimetric measurements and the corresponding derivative curves in the temperature range 30–700 °C for compounds 1 (a), 2 (b), 3 (c), 4 (d), 5 (e), and 6 (f).

Table 3. Experimental and calculated weight losses (%) for compounds 1–6 at the first plateau at around 250–300 °C.

Compound	Temperature Range (°C)	Experimental Weight Loss (%)	Solvent	Calculated Weight Loss
(NBu ₄)[MnCr(C ₆ O ₄ Cl ₂) ₃ ·C ₆ H ₅ Cl (1)	30–200	10.8	1 C ₆ H ₅ Cl	10.4
(NBu ₄)[MnCr(C ₆ O ₄ Cl ₂) ₃ ·1.5C ₆ H ₅ Br (2)	30–250	22.0	1.5 C ₆ H ₅ Br	19.5
(NBu ₄)[MnCr(C ₆ O ₄ Cl ₂) ₃ ·C ₆ H ₅ I (3)	30–200	16.6	1 C ₆ H ₅ I	17.4
(NBu ₄)[MnCr(C ₆ O ₄ Cl ₂) ₃ ·C ₆ H ₅ CH ₃ (4)	30–290	9.7	1 C ₆ H ₅ CH ₃	8.7
(NBu ₄)[MnCr(C ₆ O ₄ Cl ₂) ₃ ·2C ₆ H ₅ CN (5)	30–250	16.8	2 C ₆ H ₅ CN	17.5
(NBu ₄)[MnCr(C ₆ O ₄ Cl ₂) ₃ ·2C ₆ H ₅ NO ₂ (6)	30–220	20.7	2 C ₆ H ₅ NO ₂	20.2

2.4. Structures of Compounds 1–6

Compounds 1–6 are isostructural to compound (NBu₄)[MnCr(C₆O₄Br₂)₃·C₆H₅Br·0.5H₂O (A), [39] as shown by their X-ray powder diffractograms (Figure 4). The unit cell parameters of compounds 1–6 (Table 4), calculated from their X-ray powder diffractograms based on the structure of A with X'Pert HighScore Plus software, [45] further confirmed the isostructurality. Interestingly, compounds 1–6 did

not show any correlation between the size and the number of the solvent molecules and the unit cell parameters, suggesting that the solvent molecules are located in the hexagonal channels rather than in the interlayer space and, therefore, they do not modify the structure.

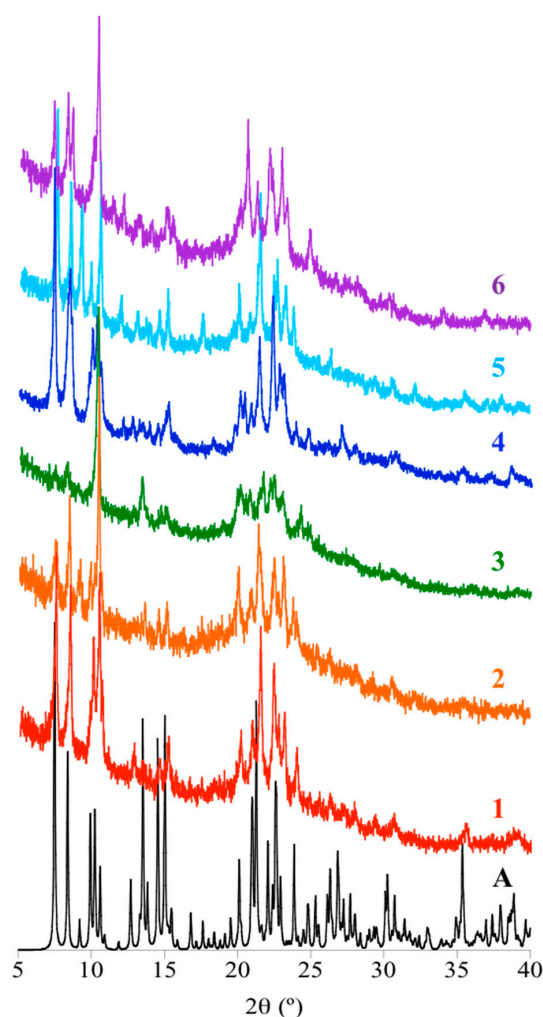


Figure 4. Simulated X-ray powder diffractogram of compound $(\text{NBu}_4)[\text{MnCr}(\text{C}_6\text{O}_4\text{Br}_2)_3]\cdot\text{C}_6\text{H}_5\text{Br}\cdot 0.5\text{H}_2\text{O}$ (A) and experimental diffractograms of compounds 1–6.

Table 4. Unit cell parameters of compounds 1–6 determined from their X-ray powder diffractograms at room temperature.

Compound	a (Å)	b (Å)	c (Å)	(°)	Volume (Å ³)
$(\text{NBu}_4)[\text{MnCr}(\text{C}_6\text{O}_4\text{Br}_2)_3]\cdot\text{C}_6\text{H}_5\text{Br}\cdot 0.5\text{H}_2\text{O}$ (A) ^a	9.9557(5)	23.6054(10)	12.2129(6)	105.187(5)	2769.9(2)
$(\text{NBu}_4)[\text{MnCr}(\text{C}_6\text{O}_4\text{Br}_2)_3]\cdot\text{C}_6\text{H}_5\text{Br}\cdot 0.5\text{H}_2\text{O}$ (A) ^b	10.104(4)	23.70(1)	12.363(5)	106.78(4)	2834.17
$(\text{NBu}_4)[\text{MnCr}(\text{C}_6\text{O}_4\text{Cl}_2)_3]\cdot\text{C}_6\text{H}_5\text{Cl}$ (1)	9.799(8)	23.76(3)	12.08(1)	104.71(8)	2719.83
$(\text{NBu}_4)[\text{MnCr}(\text{C}_6\text{O}_4\text{Cl}_2)_3]\cdot 1.5\text{C}_6\text{H}_5\text{Br}$ (2)	9.89(1)	23.66(4)	12.06(2)	103.7(1)	2740.18
$(\text{NBu}_4)[\text{MnCr}(\text{C}_6\text{O}_4\text{Cl}_2)_3]\cdot\text{C}_6\text{H}_5\text{I}$ (3)	9.71(4)	23.6(1)	12.23(6)	104.3(5)	2720.50
$(\text{NBu}_4)[\text{MnCr}(\text{C}_6\text{O}_4\text{Cl}_2)_3]\cdot\text{C}_6\text{H}_5\text{CH}_3$ (4)	9.822(7)	23.88(3)	12.09(1)	104.95(8)	2739.65
$(\text{NBu}_4)[\text{MnCr}(\text{C}_6\text{O}_4\text{Cl}_2)_3]\cdot 2\text{C}_6\text{H}_5\text{CN}$ (5)	9.887(9)	23.55(3)	12.08(1)	104.5(1)	2723.03
$(\text{NBu}_4)[\text{MnCr}(\text{C}_6\text{O}_4\text{Cl}_2)_3]\cdot 2\text{C}_6\text{H}_5\text{NO}_2$ (6)	9.58(4)	23.7(1)	11.98(6)	105.8(4)	2611.89

^a Single crystal X-ray data at 120 K [39]. ^b Determined from X-ray powder data at room temperature.

Compound A (and compounds 1–6) presents a layered structure where anionic layers of formula $[\text{MnCr}(\text{C}_6\text{O}_4\text{X}_2)_3]^-$ with X = Br (A) and Cl (1–6) alternate with cationic layers of NBu_4^+ cations (Figure 5a). The interlayer distance is 8.7 Å. The anionic layers show the classical honeycomb structure with Mn(II) and Cr(III) ions alternating in the vertex of the hexagons and the anilato ligands in the

sides (Figure 5b). The benzene derivative solvent molecules are located in the hexagonal channels formed by the eclipsed packing of the honeycomb layers (Figure 5c) and show strong π - π interactions with the anilato rings with an interplane angle of 6.95° , a centroid-centroid distance of 3.870 \AA , and a shift distance of 1.425 \AA (Figure 5d). The Br...Br distances between the Br atom of the $\text{C}_6\text{H}_5\text{Br}$ molecule and the closest bromanilato ligands are 3.82 and 3.90 \AA , only slightly above the sum of the van der Waals radii (3.72 \AA).

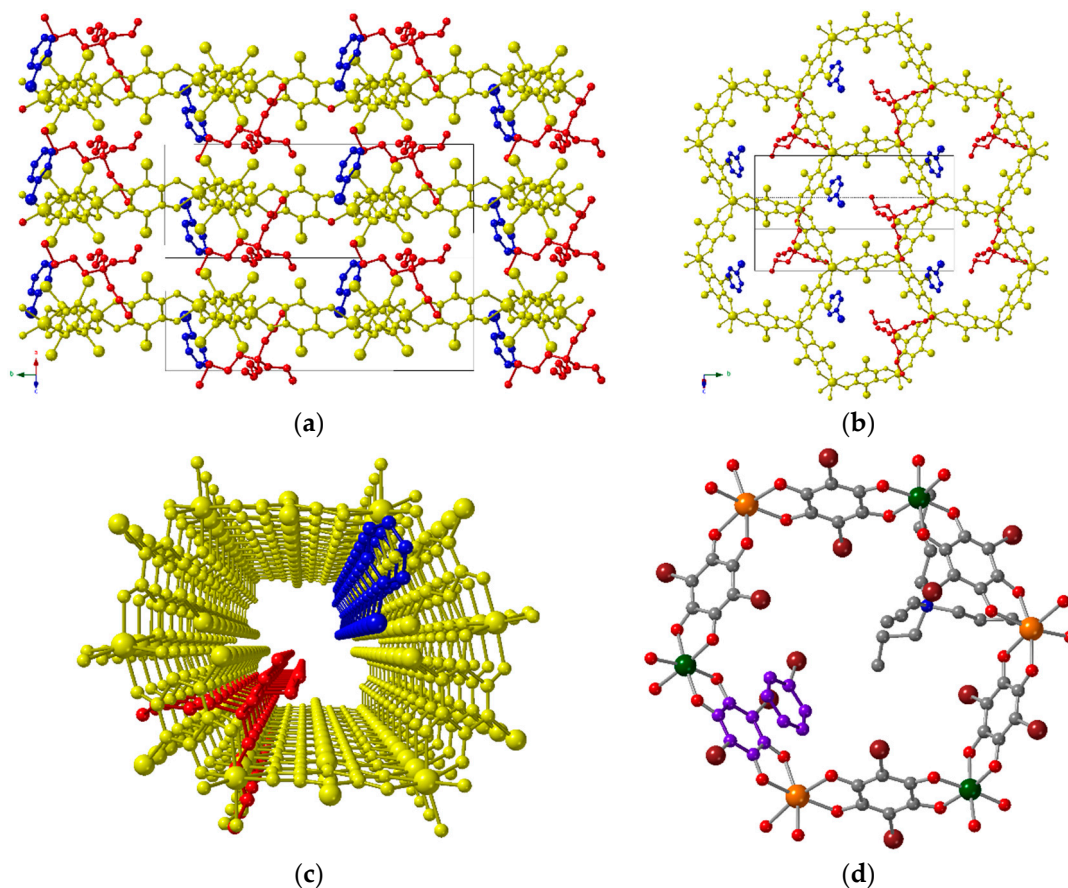


Figure 5. Structure of $(\text{NBu}_4)[\text{MnCr}(\text{C}_6\text{O}_4\text{Br}_2)_3] \cdot \text{C}_6\text{H}_5\text{Br} \cdot 0.5\text{H}_2\text{O}$ (A). (a) Side view of the alternating cationic (in red) and anionic (in yellow) layers. The solvent molecules are depicted in blue. (b) Top view of the honeycomb layer [same color code as in (a)]. (c) Perspective view of the hexagonal channels [same color code as in (a)]. (d) View of one hexagon showing the π - π interactions between the aromatic ring and one anilato ring (in purple). Color code: Mn = orange, Cr = dark green, C = grey, O = red, N = dark blue, and Br = brown. The H atoms were omitted for clarity.

2.5. Magnetic Properties

As expected, compounds 1–6 show quite similar magnetic properties, although, as we note below, there are slight differences in the ordering temperatures and the coercive fields depending on the solvent inserted in the hexagonal channels. All compounds show $\chi_m T$ values at room temperature in the range 6.25 – $6.35 \text{ cm}^3 \text{ K mol}^{-1}$ (Table 5 and Figure 6a)—very close to the calculated spin only values for $S = 3/2$ Cr(III) and $S = 5/2$ high spin Mn(II) ions [χ_m is the molar magnetic susceptibility per Mn(II)Cr(III) couple]. These $\chi_m T$ values show a continuous smooth decrease on cooling the samples and reach minimum values at around 20 K , followed by a sharp increase at around 12 K (inset Figure 6a). This behavior indicates the presence of a ferrimagnetic Mn–Cr coupling in all the samples, as observed in all the previously characterized $[\text{MnCr}(\text{C}_6\text{O}_4\text{X}_2)_3]^-$ lattices (Table 1). At *ca.* 10 K , all the samples show a maximum in $\chi_m T$, followed by an abrupt decrease due to the saturation effects of χ_m at low temperatures (Figure 6b). The sharp increase observed at *ca.* 10 – 12 K suggests the onset of a long range

ferrimagnetic ordering, in agreement with the sharp increase observed in the thermal variation of χ_m at *ca.* 10–11 K in all compounds (inset in Figure 6b).

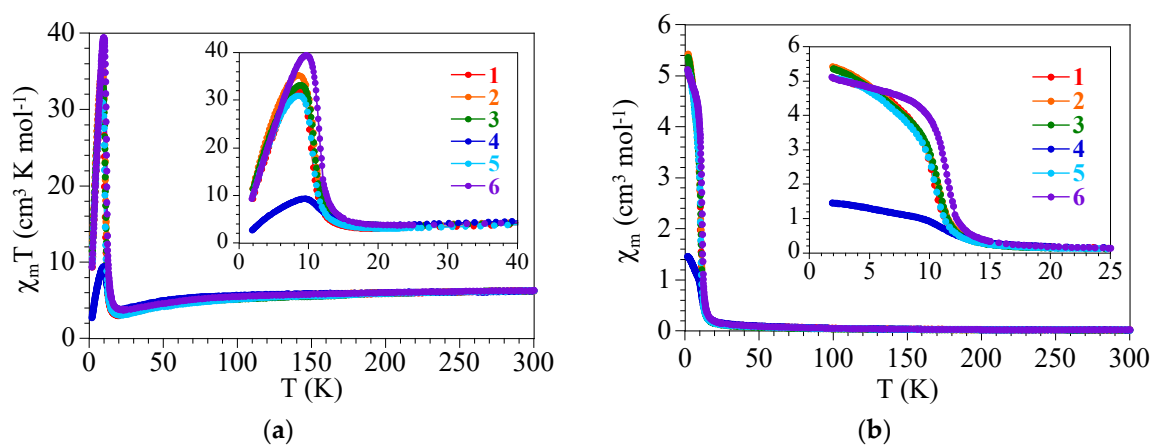


Figure 6. (a) Thermal variation of the $\chi_m T$ product (a) and χ_m (b) for compounds 1–6. Insets show zooms of the low temperature regions.

The isothermal magnetization cycles at 2 K of all the samples provide a further confirmation of the long range ferrimagnetic ordering (Figure 7). Thus, these measurements show a sharp increase of the magnetization at low fields and hysteresis cycles for all compounds with coercive fields in the range 16.2–56.2 mT (Figure 7b and Table 5). The magnetization values at 5 T in all cases are close to 2.1–2.2 μ_B (Figure 7a and Table 5), which is the expected value for a ferrimagnetic coupling between the $S = 3/2$ and $5/2$ of the Cr(III) and the Mn(II) ions of the lattice. Moreover, at high fields, the magnetization shows a linear smooth increase, further confirming the ferrimagnetic coupling in compounds 1–6.

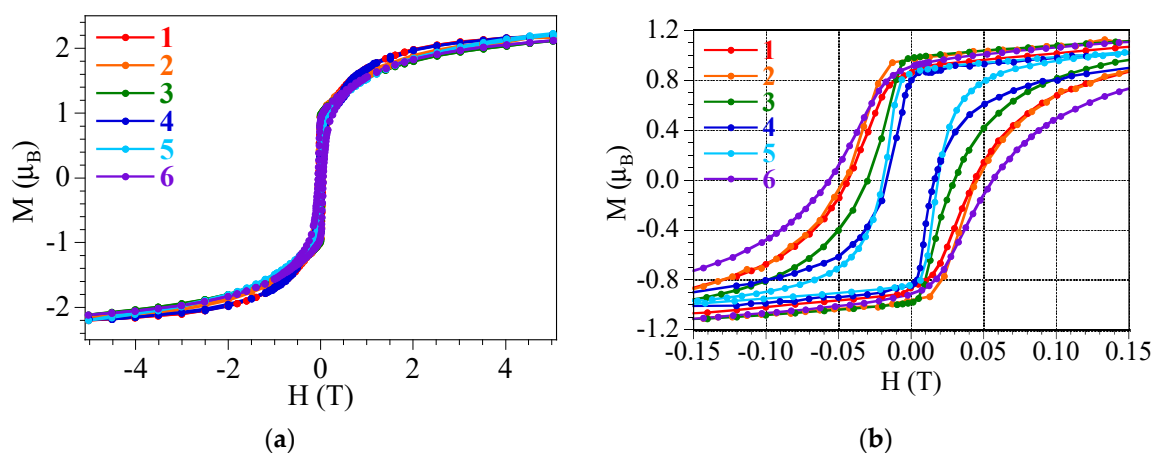


Figure 7. (a) Isothermal magnetization cycles at 2 K for compounds 1–6. (b) The low field region.

Table 5. Magnetic properties of compounds 1–6.

Compound	$\chi_m T$ @ 300 K ($\text{cm}^3 \text{K mol}^{-1}$)	T_c (K)	M @ 5 T (μ_B)	H_c (mT)
(NBu ₄)[MnCr(C ₆ O ₄ Cl ₂) ₃]·C ₆ H ₅ Cl (1)	6.29	10.4	2.20	43.7
(NBu ₄)[MnCr(C ₆ O ₄ Cl ₂) ₃]·1.5C ₆ H ₅ Br (2)	6.22	10.7	2.15	44.7
(NBu ₄)[MnCr(C ₆ O ₄ Cl ₂) ₃]·C ₆ H ₅ I (3)	6.26	11.0	2.11	30.2
(NBu ₄)[MnCr(C ₆ O ₄ Cl ₂) ₃]·C ₆ H ₅ CH ₃ (4)	6.26	9.8	2.20	16.2
(NBu ₄)[MnCr(C ₆ O ₄ Cl ₂) ₃]·2C ₆ H ₅ CN (5)	6.27	10.8	2.20	19.3
(NBu ₄)[MnCr(C ₆ O ₄ Cl ₂) ₃]·2C ₆ H ₅ NO ₂ (6)	6.30	11.2	2.12	56.2

A further confirmation of the long range ferrimagnetic order and a more precise determination of the ordering temperatures was obtained with magnetic susceptibility measurements in the presence of an alternating magnetic field (AC measurements). These measurements show, in all cases, a sharp peak in the in-phase (χ'_m) and in the out-of-phase (χ''_m) signals that does not change with the frequency (Figure 8), confirming the presence of a long range order at low temperatures in all cases. The ordering temperatures, determined as the temperature where χ''_m become non-zero, are all in the range 9.8–11.2 K (Table 5). These values are similar to those observed in most of the reported $[\text{MnCr}(\text{C}_6\text{O}_4\text{X}_2)_3]^-$ lattices (Table 1).

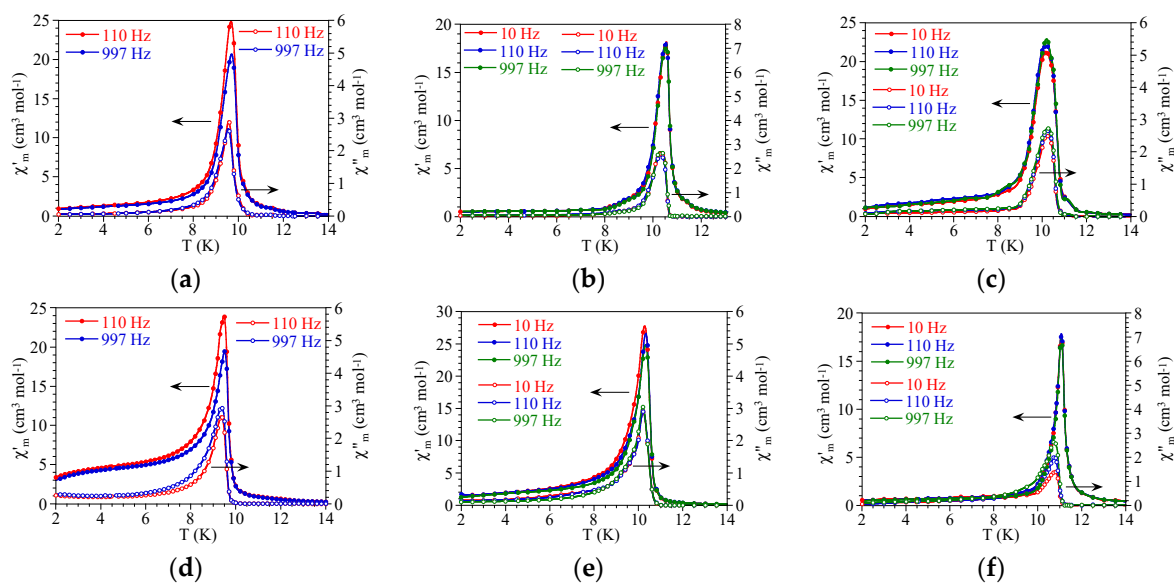


Figure 8. Thermal variation of the in-phase (χ'_m , left scales, filled symbols) and the out-of-phase (χ''_m , right scales, empty symbols) of compounds 1 (a), 2 (b), 3 (c), 4 (d), 5 (e), and 6 (f) at different frequencies.

In order to compare the ordering temperatures (T_c) of compounds 1–6, we have plotted the thermal variation of χ'_m and χ''_m at a fixed frequency (110 Hz) for all compounds (Figure 9). We can see that, even if the differences in some cases are very small, the order of T_c is: $\text{C}_6\text{H}_5\text{NO}_2$ (6) > $\text{C}_6\text{H}_5\text{I}$ (3) \approx $\text{C}_6\text{H}_5\text{CN}$ (5) > $\text{C}_6\text{H}_5\text{Br}$ (2) > $\text{C}_6\text{H}_5\text{Cl}$ (1) > $\text{C}_6\text{H}_5\text{CH}_3$ (4) (Table 5).

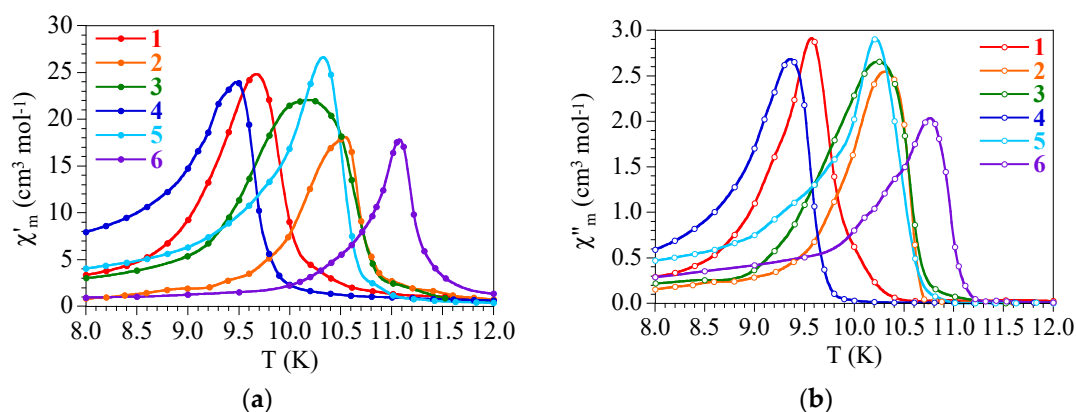


Figure 9. (a) Thermal variation of χ'_m (a) and χ''_m (b) at 110 Hz for compounds 1–6.

Although we do not have details of the crystal structure, we can assume that, in all cases, the solvent molecules (between one and two per hexagonal cavity) must interact via strong π – π stacking with the anilato rings. This assumption is supported by the similar unit cell parameters determined

from the X-ray powder diffractograms (Table 4). If the solvent molecules were located out of the hexagonal cavities (i.e., in the interlayer space), then the a and the c parameters and the unit cell volume (that are determined by the interlayer space) would be quite different in compounds 1–6, in contrast with the experimental data. Since T_c depends on the magnetic coupling through the anilato ring, and this coupling depends on the electron density of the anilato rings, [23] we can presume that the differences in T_c reflect the differences in the electron density of the anilato rings (since the six compounds contain the same anilato-type ligand). This modulation of T_c with the electron density on the anilato ring was also observed in the closely related series $(\text{NBu}_4)[\text{MnCr}(\text{C}_6\text{O}_4\text{X}_2)_3]$ with $\text{X} = \text{H}, \text{Cl}, \text{Br}$ and I [23]. On one hand, the sequence observed for the halobenzene derivatives ($\text{C}_6\text{H}_5\text{I} > \text{C}_6\text{H}_5\text{Br} > \text{C}_6\text{H}_5\text{Cl}$) agrees with the idea that the aromatic ring in $\text{C}_6\text{H}_5\text{Cl}$ had less electron density and, accordingly, donates less electron density to the anilato ring, resulting in a weaker magnetic coupling and a lower T_c . On the other hand, the higher values observed for the $\text{C}_6\text{H}_5\text{CN}$ and $\text{C}_6\text{H}_5\text{NO}_2$ derivatives may be attributed to the fact that there are two aromatic molecules per hexagon in these two compounds. The only compound that do not follow the expected trend is the $\text{C}_6\text{H}_5\text{CH}_3$ derivative (4). Since the $-\text{CH}_3$ group is electron donating, it should present a higher T_c than the three halobenzene derivatives. A possible reason to explain this anomaly might be the formation of H-bonds between the $-\text{CH}_3$ group and the oxygen atoms or the chlorine atoms of the chloranilato ligand. The formation of such H-bonds has already been observed in other related Ln(III)-containing anilato-based lattices [34]. The higher temperature needed in the thermogravimetric measurements to release the toluene molecule in this compound agrees with this idea. These H-bonds are expected to shift the aromatic ring of the toluene molecule from its ideal position, reducing the π - π stacking with the anilato ring and, accordingly, the electron density on the anilato ring and T_c .

The idea that the solvent molecules play an important role in T_c is further supported by the fact that the de-solvated compound $(\text{NBu}_4)[\text{MnCr}(\text{C}_6\text{O}_4\text{Cl}_2)_3]$ (**B**) [23] shows an ordering temperature of 5.5 K (Table 1), well below the observed ones in compounds 1–6. Although compound **B** has a slightly different structure (the honeycomb layers are alternated, and the hexagonal rings are completely planar), the lower value of T_c in the de-solvated compound suggests that the presence of the solvent molecules increases the electron density in the anilato rings and, accordingly, the magnetic coupling and the ordering temperatures. In fact, preliminary measurements performed on compound 6 after heating the sample at 400 K under vacuum to remove the PhNO_2 molecules show a slight decrease in T_c (and an important decrease of the coercive field), further supporting the idea that the solvent molecules are responsible for the fine tuning of T_c .

Despite compounds 1–6 show very close unit cell parameters (Table 4), we cannot discard that, besides the electronic effect, the solvent molecules exert a very tiny structural effect. Although with more important structural changes, this structural effect has already been observed in compounds $(\text{NMe}_2\text{H}_2)_2[\text{Fe}_2(\text{C}_6\text{O}_4\text{Cl}_2)_3] \cdot 2\text{H}_2\text{O} \cdot 6\text{DMF}$ [27] and $(\text{Et}(i\text{-Pr})_2\text{NH})[\text{MnCr}(\text{C}_6\text{O}_4\text{Br}_2)_3] \cdot \text{H}_2\text{O} \cdot 0.5\text{CHCl}_3$ [28].

3. Experimental Section

3.1. Starting Materials

Chloranilic acid ($\text{H}_2\text{C}_6\text{O}_4\text{Cl}_2$), $\text{MnCl}_2 \cdot 4\text{H}_2\text{O}$, and all the used solvents ($\text{C}_6\text{H}_5\text{Cl}$, $\text{C}_6\text{H}_5\text{Br}$, $\text{C}_6\text{H}_5\text{I}$, $\text{C}_6\text{H}_5\text{CH}_3$, $\text{C}_6\text{H}_5\text{CN}$, and $\text{C}_6\text{H}_5\text{NO}_2$) are commercially available and were used as received without further purification. The precursor salt $(\text{NBu}_4)_3[\text{Cr}(\text{C}_6\text{O}_4\text{Cl}_2)_3]$ was prepared as reported in the literature [23].

3.2. Synthesis of $(\text{NBu}_4)[\text{MnCr}(\text{C}_6\text{O}_4\text{Cl}_2)_3] \cdot \text{C}_6\text{H}_5\text{Cl}$ (**1**)

Compound **1** was prepared by carefully layering, at room temperature, a solution of $(\text{NBu}_4)_3[\text{Cr}(\text{C}_6\text{O}_4\text{Cl}_2)_3]$ (70 mg, 0.05 mmol) in acetonitrile (10 mL) on top of a solution of $\text{MnCl}_2 \cdot 4\text{H}_2\text{O}$ (40 mg, 0.2 mmol) in 4 mL of MeOH and 6 mL of chlorobenzene. An intermediate layer with a mixture of methanol:chlorobenzene (8:1) was used in order to slow down the diffusion. The solution was

allowed to stand for two weeks to obtain a dark powder, which was filtered and air-dried. FT-IR (ν/cm^{-1} , KBr pellet): 3440 (vs), 2960 (m), 2930 (w), 2873 (w), 1608 (m), 1497 (vs), 1360 (vs), 1306 (w), 1008 (w), 858 (s), 743 (m), 700 (w), 685 (w), 628 (s), 578 (m), 513 (s), 465 (m).

Anal. Calcd. (%) for $\text{C}_{40}\text{H}_{41}\text{Cl}_7\text{CrMnNO}_{12}$: C, 44.37; N, 1.29; H, 3.82. Found (%): C, 43.74; N, 1.21; H, 3.99. Elemental ratio estimated by electron probe microanalysis (EPMA): found: Mn:Cr:Cl = 11.5:11.4:77.1 (1.0:1.0:6.8). Calc. for $\text{C}_{40}\text{H}_{41}\text{Cl}_7\text{CrMnNO}_{12}$: Mn:Cr:Cl = 1:1:7.

3.3. Synthesis of $(\text{NBu}_4)[\text{MnCr}(\text{C}_6\text{O}_4\text{Cl}_2)_3]\cdot 1.5\text{C}_6\text{H}_5\text{Br}$ (2)

Compound **2** was prepared as **1** but using bromobenzene instead of chlorobenzene. The solution was allowed to stand for two weeks to obtain a dark powder, which was filtered and air-dried. FT-IR (ν/cm^{-1} , KBr pellets): 3420 (vs), 2961 (m), 2930 (w), 2872 (w), 1608 (m), 1497 (vs), 1361 (vs), 1305 (w), 1066 (w), 1006 (m), 856 (s), 736 (m), 683 (w), 670 (w), 626 (s), 576 (m), 513 (s), 463 (m).

Anal. Calcd. (%) for $\text{C}_{43}\text{H}_{43.5}\text{Br}_{1.1}\text{Cl}_6\text{CrMnNO}_{12}$: C, 42.83; N, 1.16; H, 3.63. Found (%): C, 42.82; N, 1.05; H, 3.45. Elemental ratio estimated by electron probe microanalysis (EPMA): found: Mn:Cr:Cl:Br = 9.9:10.2:63.4:16.4 (1.0:1.0:6.4:1.6). Calc. for $\text{C}_{43}\text{H}_{43.5}\text{Br}_{1.5}\text{Cl}_6\text{CrMnNO}_{12}$: Mn:Cr:Cl:Br = 1:1:6:1.5.

3.4. Synthesis of $(\text{NBu}_4)[\text{MnCr}(\text{C}_6\text{O}_4\text{Cl}_2)_3]\cdot \text{C}_6\text{H}_5\text{I}$ (3)

Compound **3** was prepared as **1** but using iodobenzene instead of chlorobenzene. The solution was allowed to stand for two weeks to obtain a dark powder, which was filtered and air-dried. FT-IR (ν/cm^{-1} , KBr pellets): 3443 (vs), 2961 (m), 2926 (w), 2872 (w), 1606 (m), 1496 (vs), 1363 (vs), 1306 (w), 1011 (m), 858 (s), 730 (m), 683 (w), 666 (w), 627 (s), 577 (m), 513 (s), 458 (s).

Anal. Calcd. (%) for $\text{C}_{40}\text{H}_{41}\text{ICl}_6\text{CrMnNO}_{12}$: C, 40.91; N, 1.19; H, 3.52. Found (%): C, 39.40; N, 0.99; H, 3.99.

3.5. Synthesis of $(\text{NBu}_4)[\text{MnCr}(\text{C}_6\text{O}_4\text{Cl}_2)_3]\cdot \text{C}_6\text{H}_5\text{CH}_3$ (4)

Compound **4** was prepared as **1** but using toluene instead of chlorobenzene. The solution was allowed to stand for two weeks to obtain a dark powder, which was filtered and air-dried. FT-IR (ν/cm^{-1} , KBr pellets): 3440 (vs), 2961 (m), 2930 (w), 2872 (w), 1608 (m), 1497 (vs), 1361 (vs), 1305 (w), 1008 (m), 856 (s), 730 (m), 696 (w), 670 (w), 630 (s), 576 (m), 513 (s), 463 (m).

Anal. Calcd. (%) for $\text{C}_{41}\text{H}_{44}\text{Cl}_6\text{CrMnNO}_{12}$: C, 46.35; N, 1.32; H, 4.17. Found (%): C, 45.13; N, 1.12; H, 4.10.

3.6. Synthesis of $(\text{NBu}_4)[\text{MnCr}(\text{C}_6\text{O}_4\text{Cl}_2)_3]\cdot 2\text{C}_6\text{H}_5\text{CN}$ (5)

Compound **5** was prepared as **1** but using benzonitrile instead of chlorobenzene. The solution was allowed to stand for two weeks to obtain a dark powder, which was filtered and air-dried. FT-IR (ν/cm^{-1} , KBr pellets): 3443 (vs), 2963 (m), 2930 (w), 2873 (w), 1605 (m), 1497 (vs), 1360 (vs), 1306 (w), 1005 (m), 858 (s), 755 (m), 733 (w), 686 (w), 627 (s), 577 (m), 547 (w), 513 (s), 461 (m).

Anal. Calcd. (%) for $\text{C}_{44.5}\text{H}_{44.5}\text{Cl}_6\text{CrMnN}_{2.5}\text{O}_{12}$: C, 49.00; N, 3.57; H, 3.94. Found (%): C, 47.00; N, 3.16; H, 3.01.

3.7. Synthesis of $(\text{NBu}_4)[\text{MnCr}(\text{C}_6\text{O}_4\text{Cl}_2)_3]\cdot 2\text{C}_6\text{H}_5\text{NO}_2$ (6)

Compound **6** was prepared as **1** but using nitrobenzene instead of chlorobenzene. The solution was allowed to stand for two weeks to obtain a dark powder, which was filtered and air-dried. FT-IR (ν/cm^{-1} , KBr pellets): 3443 (vs), 2961 (m), 2934 (w), 2872 (w), 1606 (m), 1496 (vs), 1360 (vs), 1306 (w), 1005 (m), 858 (s), 791 (w), 736 (w), 705 (m), 683 (w), 666 (w), 625 (s), 577 (m), 513 (s), 463 (m).

Anal. Calcd. (%) for $\text{C}_{43}\text{H}_{43.5}\text{Cl}_6\text{CrMnN}_{2.5}\text{O}_{15}$: C, 45.42; N, 3.45; H, 3.81. Found (%): C, 44.56; N, 3.21; H, 3.42.

3.8. Magnetic Measurements

Magnetic measurements were performed with a Quantum Design MPMS-XL-5 SQUID magnetometer (San Diego, CA, USA) with an applied magnetic field of 0.1 T (0.5 T for compound **4**) in the 2–300 K temperature range on polycrystalline samples of all the compounds with masses of 7.514, 3.824, 9.056, 1.002, 5.932, and 4.998 mg for compounds **1–6**, respectively. The isothermal magnetization hysteresis measurements were done with fields from –5 to 5 Tesla at 2 K. AC susceptibility measurements were performed on the same samples with an AC field of 0.395 mT in the temperature range 2–14 K and in the frequency range 10–1000 Hz. Susceptibility data were corrected for the sample holder and for the diamagnetic contribution of the salts using Pascal's constants [46].

3.9. X-ray Powder Diffraction

The X-ray powder diffractograms were collected on polycrystalline samples of compounds **1–6** using a 0.5 mm glass capillary that was mounted and aligned on an Empyrean PANalytical powder diffractometer using $\text{CuK}\alpha$ radiation ($\lambda = 1.54177 \text{ \AA}$). A total of six scans were collected at room temperature in the 2θ range $5\text{--}40^\circ$ and merged in a single diffractogram.

3.10. Physical Properties

FT-IR spectra were performed on KBr pellets and collected with a Bruker Equinox 55 spectrophotometer. C, H, and N analyses were performed with a Thermo Electron CHNS Flash 2000 analyser and with a Carlo Erba mod. EA1108 CHNS analyzer. The Mn:Cr:Cl:X ratios (X = Cl in **1** and Br in **2**) of the bulk samples were estimated by electron probe microanalysis (EPMA) performed in a Philips SEM XL30 equipped with an EDAX DX-4 microprobe. Thermogravimetric (TG) measurements were performed in Pt crucibles with a TA instruments TGA 550 thermobalance equipped with an autosampler. The TG measurements were done in the $30\text{--}700^\circ\text{C}$ temperature range at $10^\circ\text{C}/\text{min}$ under a N_2 flux of 60 mL/min.

4. Conclusions

The series of six compounds formulated as $(\text{NBu}_4)[\text{MnCr}(\text{C}_6\text{O}_4\text{Cl}_2)_3]\cdot n\text{G}$ with $n = 1$ for $\text{G} = \text{C}_6\text{H}_5\text{Cl}$ (**1**), $\text{C}_6\text{H}_5\text{I}$ (**3**), $\text{C}_6\text{H}_5\text{CH}_3$ (**4**), $n = 1.5$ for $\text{C}_6\text{H}_5\text{Br}$ (**2**), and $n = 2$ for $\text{G} = \text{C}_6\text{H}_5\text{CN}$ (**5**), and $\text{C}_6\text{H}_5\text{NO}_2$ (**6**) show that it is possible to prepare a complete series of isostructural 2D ferrimagnets by simply changing the solvent molecules. This series presents the classical honeycomb 2D lattice with an eclipsed packing of the layers giving rise to hexagonal channels and shows long range ferrimagnetic order with T_c ranging from 9.8 to 11.2 K. Interestingly, this fine modulation of T_c seems to be related to the electronic character and the number of solvent molecules that enter in the hexagonal channels of these 2D ferrimagnets. We have also prepared the corresponding bromanilato series with the same solvent molecules. Preliminary magnetic measurements show that they are also ferrimagnets with very similar T_c and with a very close sequence of ordering temperatures, further supporting the above results. Work is in progress to complete these series with other aromatic (and not aromatic) solvents and for other anilato ligands and even metal ions. Finally, attempts to remove and/or exchange the different solvent molecules are under investigation. Preliminary results suggest that it is indeed possible to exchange and even to remove the solvents molecules and, as expected, the exchanged and the evacuated compounds slightly modify their ordering temperatures.

Author Contributions: Conceptualization, S.B.; Data curation, C.M.-H., S.B. and C.J.G.-G.; Formal analysis, C.M.-H., S.B. and C.J.G.-G.; Funding acquisition, C.J.G.-G.; Investigation, C.M.-H., S.B. and C.J.G.-G.; Methodology, C.M.-H. and S.B.; Project administration, C.J.G.-G.; Supervision, S.B.; Visualization, S.B.; Writing—original draft, C.J.G.-G.; Writing—review & editing, S.B.

Funding: This research was funded by the Spanish MINECO (project CTQ2017-87201-P AEI/FEDER, UE). C.M.-H. and a pre-doctoral grant from the University of Valencia.

Acknowledgments: Thanks for the funding from the Spanish MINECO (project CTQ2017-87201-P AEI/FEDER, UE). C.M.-H. and the University of Valencia for a pre-doctoral grant.

Conflicts of Interest: The authors declare no conflict of interest.

References

1. Miller, J.S.; Gatteschi, D. Molecule-based magnets. *Chem. Soc. Rev.* **2011**, *40*, 3065–3066. [[CrossRef](#)] [[PubMed](#)]
2. Verdaguer, M.; Bleuzen, A.; Marvaud, V.; Vaissermann, J.; Seuleiman, M.; Desplanches, C.; Scullier, A.; Train, C.; Garde, R.; Gelly, G.; et al. Molecules to build solids: High TC molecule-based magnets by design and recent revival of cyano complexes chemistry. *Coord. Chem. Rev.* **1999**, *190*, 1023–1047. [[CrossRef](#)]
3. Ohba, M.; Ōkawa, H. Synthesis and magnetism of multi-dimensional cyanide-bridged bimetallic assemblies. *Coord. Chem. Rev.* **2000**, *198*, 313–328. [[CrossRef](#)]
4. Culp, J.T.; Park, J.H.; Frye, F.; Huh, Y.D.; Meisel, M.W.; Talham, D.R. Magnetism of metal cyanide networks assembled at interfaces. *Coord. Chem. Rev.* **2005**, *249*, 2642–2648. [[CrossRef](#)]
5. Weihe, H.; Güdel, H.U. Magnetic Exchange Across the Cyanide Bridge. *Comments Inorg. Chem.* **2000**, *22*, 75–103. [[CrossRef](#)]
6. Ruiz, E.; Rodríguez-Forteza, A.; Alvarez, S.; Verdaguer, M. Is it possible to get high TC magnets with Prussian blue analogues? A theoretical prospect. *Chem. Eur. J.* **2005**, *11*, 2135–2144. [[CrossRef](#)] [[PubMed](#)]
7. Sato, O.; Iyoda, T.; Fujishima, A.; Hashimoto, K. Photoinduced Magnetization of a Cobalt-Iron Cyanide. *Science* **1996**, *272*, 704–705. [[CrossRef](#)] [[PubMed](#)]
8. Sato, O. Switchable molecular magnets. *Proc. Jpn. Acad. Ser. B Phys. Biol. Sci.* **2012**, *88*, 213–225. [[CrossRef](#)] [[PubMed](#)]
9. Shimamoto, N.; Ohkoshi, S.; Sato, O.; Hashimoto, K. Control of Charge-Transfer-Induced Spin Transition Temperature on Cobalt-Iron Prussian Blue Analogues. *Inorg. Chem.* **2002**, *41*, 678–684. [[CrossRef](#)]
10. Miyasaka, H.; Julve, M.; Yamashita, M.; Clérac, R. Slow Dynamics of the Magnetization in One-Dimensional Coordination Polymers: Single-Chain Magnets. *Inorg. Chem.* **2009**, *48*, 3420–3437. [[CrossRef](#)] [[PubMed](#)]
11. Funck, K.E.; Hilfiger, M.G.; Berlinguette, C.P.; Shatruk, M.; Wernsdorfer, W.; Dunbar, K.R. Trigonal-Bipyramidal Metal Cyanide Complexes: A Versatile Platform for the Systematic Assessment of the Magnetic Properties of Prussian Blue Materials. *Inorg. Chem.* **2009**, *48*, 3438–3452. [[CrossRef](#)] [[PubMed](#)]
12. Ferlay, S.; Mallah, T.; Ouahes, R.; Veillet, P.; Verdaguer, M.; Ouah, R. A room-temperature organometallic magnet based on Prussian blue. *Nature* **1995**, *378*, 701–703. [[CrossRef](#)]
13. Tamaki, H.; Zhong, Z.J.; Matsumoto, N.; Kida, S.; Koikawa, M.; Achiwa, N.; Hashimoto, Y.; Okawa, H. Design of metal-complex magnets. Syntheses and magnetic properties of mixed-metal assemblies $\{N\text{Bu}_4[\text{M}(\text{ox})_3]\}_x$ ($N\text{Bu}_4^+$ = tetra(n-butyl)ammonium ion; ox^{2-} = oxalate ion; $\text{M} = \text{Mn}^{2+}, \text{Fe}^{2+}, \text{Co}^{2+}, \text{Ni}^{2+}, \text{Cu}^{2+}, \text{Zn}^{2+}$). *J. Am. Chem. Soc.* **1992**, *114*, 6974–6979. [[CrossRef](#)]
14. Mathoniere, C.; Nuttall, C.J.; Carling, S.G.; Day, P. Ferrimagnetic Mixed-Valency and Mixed-Metal Tris(oxalato)iron(III) Compounds: Synthesis, Structure, and Magnetism. *Inorg. Chem.* **1996**, *35*, 1201–1206. [[CrossRef](#)] [[PubMed](#)]
15. Clement, R.; Decurtins, S.; Gruselle, M.; Train, C. Polyfunctional two-(2D) and three-(3D) dimensional oxalate bridged bimetallic magnets. *Monatshfte Chem.* **2003**, *134*, 117–135. [[CrossRef](#)]
16. Benmansour, S.; Cerezo-Navarrete, C.; Canet-Ferrer, J.; Muñoz-Matutano, G.; Martínez-Pastor, J.; Gómez-García, C.J. A fluorescent layered oxalato-based canted antiferromagnet. *Dalton Trans.* **2018**, *47*, 11909–11916. [[CrossRef](#)] [[PubMed](#)]
17. Clemente-León, M.; Coronado, E.; Galán-Mascarós, J.R.; Gómez-García, C.J. Intercalation of decamethylferrocenium cations in bimetallic oxalate-bridged two-dimensional magnets. *Chem. Commun.* **1997**, 1727–1728.
18. Coronado, E.; Clemente-León, M.; Galán-Mascarós, J.R.; Giménez-Saiz, C.; Gómez-García, C.J.; Martínez-Ferrero, E. Design of molecular materials combining magnetic, electrical and optical properties. *J. Chem. Soc. Dalton Trans.* **2000**, 3955–3961. [[CrossRef](#)]
19. Coronado, E.; Galán-Mascarós, J.R.; Gómez-García, C.J.; Enslin, J.; Gütlich, P. Hybrid molecular magnets obtained by insertion of decamethyl-metalloccenium cations into layered, bimetallic oxalate complexes: $[\text{Z}^{\text{III}}\text{Cp}^*_2][\text{M}^{\text{II}}\text{M}^{\text{III}}(\text{ox})_3]$ ($\text{Z}^{\text{III}} = \text{Co}, \text{Fe}$; $\text{M}^{\text{III}} = \text{Cr}, \text{Fe}$; $\text{M}^{\text{II}} = \text{Mn}, \text{Fe}, \text{Co}, \text{Cu}, \text{Zn}$; $\text{ox} = \text{oxalate}$; $\text{Cp}^* = \text{pentamethylcyclopentadienyl}$). *Chem. Eur. J.* **2000**, *6*, 552–563. [[CrossRef](#)]

20. Coronado, E.; Galán-Mascarós, J.R.; Gómez-García, C.J.; Martínez-Agudo, J.M. Increasing the coercivity in layered molecular-based magnets $A[M^{II}M^{III}(ox)_3]$ ($M^{II} = Mn, Fe, Co, Ni, Cu$; $M^{III} = Cr, Fe$; $ox = oxalate$; $A = organic\ or\ organometallic\ cation$). *Adv. Mater.* **1999**, *11*, 558–561. [[CrossRef](#)]
21. Coronado, E.; Galán-Mascarós, J.R.; Gómez-García, C.J.; Martínez-Agudo, J.M.; Martínez-Ferrero, E.; Waerenborgh, J.C.; Almeida, M. Layered molecule-based magnets formed by decamethylmetalloccenium cations and two-dimensional bimetallic complexes $[M^{II}Ru^{III}(ox)_3]^{-}$ ($M^{II} = Mn, Fe, Co, Cu\ and\ Zn$; $ox = oxalate$). *J. Solid State Chem.* **2001**, *159*, 391–402. [[CrossRef](#)]
22. Coronado, E.; Galán-Mascarós, J.R.; Gómez-García, C.J.; Laukhin, V. Coexistence of ferromagnetism and metallic conductivity in a molecule-based layered compound. *Nature* **2000**, *408*, 447–449. [[CrossRef](#)] [[PubMed](#)]
23. Atzori, M.; Benmansour, S.; Mínguez Espallargas, G.; Clemente-León, M.; Abhervé, A.; Gómez-Claramunt, P.; Coronado, E.; Artizzu, F.; Sessini, E.; Deplano, P.; et al. A Family of Layered Chiral Porous Magnets Exhibiting Tunable Ordering Temperatures. *Inorg. Chem.* **2013**, *52*, 10031–10040. [[CrossRef](#)] [[PubMed](#)]
24. Mercuri, M.L.; Congiu, F.; Concas, G.; Sahadevan, S.A. Recent Advances on Anilato-Based Molecular Materials with Magnetic and/or Conducting Properties. *Magnetochem* **2017**, *3*, 17. [[CrossRef](#)]
25. Kitagawa, S.; Kawata, S. Coordination compounds of 1,4-dihydroxybenzoquinone and its homologues. Structures and properties. *Coord. Chem. Rev.* **2002**, *224*, 11–34. [[CrossRef](#)]
26. Halis, S.; Inge, A.K.; Dehning, N.; Weyrich, T.; Reinsch, H.; Stock, N. Dihydroxybenzoquinone as Linker for the Synthesis of Permanently Porous Aluminum Metal–Organic Frameworks. *Inorg. Chem.* **2016**, *55*, 7425–7431. [[CrossRef](#)]
27. Jeon, I.R.; Negru, B.; Van Duyne, R.P.; Harris, T.D. A 2D Semiquinone Radical-Containing Microporous Magnet with Solvent-Induced Switching from $T_c = 26$ to 80 K. *J. Am. Chem. Soc.* **2015**, *137*, 15699–15702. [[CrossRef](#)]
28. Palacios-Corella, M.; Fernández-Espejo, A.; Bazaga-García, M.; Losilla, E.R.; Cabeza, A.; Clemente-León, M.; Coronado, E. Influence of Proton Conducting Cations on the Structure and Properties of 2D Anilate-Based Magnets. *Inorg. Chem.* **2017**, *56*, 13865–13877. [[CrossRef](#)]
29. Riley, P.E.; Haddad, S.F.; Raymond, K.N. Preparation of praseodymium(III) chloranilate and the crystal structures of $Pr_2(C_6Cl_2O_4)_3 \cdot 8C_2H_5OH$ and $Na_3[C_6H_2O(OH)(SO_3)_2] \cdot H_2O$. *Inorg. Chem.* **1983**, *22*, 3090–3096. [[CrossRef](#)]
30. Christian, R. Complexes with substituted 2,5-dihydroxy-p-benzoquinones: The inclusion compounds $[Y(H_2O)_3]_2(C_6Cl_2O_4)_3 \cdot 6H_2O$ and $[Y(H_2O)_3]_2(C_6Br_2O_4)_3 \cdot 6H_2O$. *Mater. Res. Bull.* **1987**, *22*, 1483–1491.
31. Abrahams, B.F.; Coleiro, J.; Hoskins, B.F.; Robson, R. Gas hydrate-like pentagonal dodecahedral $M_2(H_2O)_{18}$ cages ($M = lanthanide\ or\ Y$) in 2,5-dihydroxybenzoquinone-derived coordination polymers. *Chem. Commun.* **1996**, 603–604. [[CrossRef](#)]
32. Coleiro, J.; Ha, K.; Orchard, S.D.; Robson, R.; Abrahams, B.F.; Hoskins, B.F. Dihydroxybenzoquinone and chloranilic acid derivatives of rare earth metals. *J. Chem. Soc. Dalton Trans.* **2002**, 1586–1594.
33. Benmansour, S.; Pérez-Herráez, I.; López-Martínez, G.; Gómez-García, C.J. Solvent-modulated structures in anilato-based 2D coordination polymers. *Polyhedron* **2017**, *135*, 17–25. [[CrossRef](#)]
34. Benmansour, S.; Pérez-Herráez, I.; Cerezo-Navarrete, C.; López-Martínez, G.; Martínez Hernández, C.; Gómez-García, C.J. Solvent-modulation of the structure and dimensionality in lanthanoid-anilato coordination polymers. *Dalton Trans.* **2018**, *47*, 6729–6741. [[CrossRef](#)] [[PubMed](#)]
35. Benmansour, S.; Hernández-Paredes, A.; Gómez-García, C.J. Effect of the lanthanoid-size on the structure of a series of lanthanoid-anilato 2-D lattices. *J. Coord. Chem.* **2018**, *71*, 845–863. [[CrossRef](#)]
36. Gómez-Claramunt, P.; Benmansour, S.; Hernández-Paredes, A.; Cerezo-Navarrete, C.; Rodríguez-Fernández, C.; Canet-Ferrer, J.; Cantarero, A.; Gómez-García, C.J. Tuning the Structure and Properties of Lanthanoid Coordination Polymers with an Asymmetric Anilato Ligand. *Magnetochem* **2018**, *4*, 6.
37. Benmansour, S.; Hernández-Paredes, A.; Gómez-García, C.J. Two Dimensional Magnetic Coordination Polymers Formed by Lanthanoids and Chlorocyananilato. *Magnetochem* **2018**, *4*, 58. [[CrossRef](#)]
38. Ashoka Sahadevan, S.; Monni, N.; Abhervé, A.; Marongiu, D.; Sarritzu, V.; Sestu, N.; Saba, M.; Mura, A.; Bongiovanni, G.; Cannas, C.; et al. Nanosheets of Two-Dimensional Neutral Coordination Polymers Based on Near-Infrared-Emitting Lanthanides and a Chlorocyananilate Ligand. *Chem. Mater.* **2018**, *30*, 6575–6586. [[CrossRef](#)]

39. Gómez-Claramunt, P. Anilato-Based Multifunctional Molecular Materials. Ph.D. Thesis, University of Valencia, Valencia, Spain, 2018.
40. Abhervé, A.; Verneret, M.; Clemente-León, M.; Coronado, E.; Gómez-García, C.J. One-Dimensional and Two-Dimensional Anilate-Based Magnets with Inserted Spin-Crossover Complexes. *Inorg. Chem.* **2014**, *53*, 12014–12026.
41. Abhervé, A.; Mañas-Valero, S.; Clemente-León, M.; Coronado, E. Graphene related magnetic materials: Micromechanical exfoliation of 2D layered magnets based on bimetallic anilate complexes with inserted $[\text{Fe}^{\text{III}}(\text{acac}_2\text{-trien})]^+$ and $[\text{Fe}^{\text{III}}(\text{sal}_2\text{-trien})]^+$ molecules. *Chem. Sci.* **2015**, *6*, 4665–4673. [[CrossRef](#)]
42. Benmansour, S.; Abhervé, A.; Gómez-Claramunt, P.; Vallés-García, C.; Gómez-García, C.J. Nanosheets of Two-Dimensional Magnetic and Conducting Fe(II)/Fe(III) Mixed-Valence Metal–Organic Frameworks. *ACS Appl. Mater. Interfaces* **2017**, *9*, 26210–26218. [[CrossRef](#)] [[PubMed](#)]
43. Sahadevan, S.A.; Abhervé, A.; Monni, N.; Sáenz, D.P.; Galán-Mascarós, J.R.; Waerenborgh, J.C.; Vieira, B.J.C.; Auban-Senzier, P.; Pillet, S.; Bendeif, E.; et al. Conducting Anilate-Based Mixed-Valence Fe(II)Fe(III) Coordination Polymer: Small-Polaron Hopping Model for Oxalate-Type Fe(II)Fe(III) 2D Networks. *J. Am. Chem. Soc.* **2018**, *140*, 12611–12621. [[CrossRef](#)] [[PubMed](#)]
44. Martínez-Hernández, C.; Benmansour, S.; Gómez-García, C.J. Modulation of the ordering temperature in anilato-based magnets. *Polyhedron* **2019**, in press. [[CrossRef](#)]
45. *PANalytical X'Pert HighScore Plus*; PANalytical I. V.: Almelo, The Netherlands, 2012.
46. Bain, G.A.; Berry, J.F. Diamagnetic Corrections and Pascal's Constants. *J. Chem. Educ.* **2008**, *85*, 532. [[CrossRef](#)]



© 2019 by the authors. Licensee MDPI, Basel, Switzerland. This article is an open access article distributed under the terms and conditions of the Creative Commons Attribution (CC BY) license (<http://creativecommons.org/licenses/by/4.0/>).